scientific reports

Check for updates

OPEN

# Ultrasound imaging of the perithyroid fascial space: a comparative analysis with anatomical correlations

Ying Wei[1], Zhen-long Zhao[1], Yun Niu[2], Li-li Peng[1], Yan Li[1] & Ming-an Yu[1]✉

**This study aims to examine the ultrasonic characteristics of perithyroid fascial spaces following in vivo hydrodissection, validating their visualization through a comparative analysis with anatomical references. A retrospective review was conducted on data from 2390 patients (631 males and 1759 females, median age 46 years, 25–75% interquartile range 26–69 years) who underwent microwave ablation for thyroid tumors, including 1436 benign nodules and 954 papillary thyroid carcinomas. Detailed descriptions of perithyroid fascial spaces and the hydrodissection strategy were provided. Ultrasonic characteristics of fascial spaces during hydrodissection were documented and systematically compared with anatomical references. Hydrodissection was successfully performed in all cases according to the protocol. Isolating fluid was injected into classic anatomical spaces: anterior cervical (58.5%), pretracheal (71.8%, including Berry's ligament in 196 cases), retropharyngeal (43.7%), and carotid (1.2%). Additionally, US revealed two new spaces—perilymphatic (4.1%) and tracheoesophageal groove (3.7%)—with corresponding anatomical structures. The US-identified fascial structures aligned with their anatomical positions and distribution. US-guided hydrodissection facilitates the visualization of the fascial space, making it possible to study the microenvironment physiology and pathology of fascia in vivo.**

**Keywords** Thyroid, Fascial space, Hydrodissection, Ultrasound

Fascia, originating from the mesoderm, primarily comprises fibrous connective tissue and fat, creating a pervasive network throughout the body[1]. Traditionally defined as organized connective tissue forming sheets or sheaths around structures[2–4], recent research, as highlighted by the International Fascia Research Congress, has redefined fascia as the "three-dimensional continuum of soft, collagen-containing, loose and dense fibrous connective tissues that permeate the body"[5]. This fascial system interpenetrates and envelops all organs, muscles, bones, and nerve fibers, providing the body with a functional structure and an environment conducive to the integrated operation of all bodily systems.

As a tensional continuous fibrillar network, fascia forms distinct fascial spaces in various regions. The thyroid is enveloped by several fasciae and unique fascial spaces, each holding specific anatomical, physiological, and pathological significance. In the era of modern precision medicine, a comprehensive understanding of these fascial spaces is imperative for surgeons to ensure safe operations. It also enables access to previously hard-to-reach areas in endoscopic and robotic surgery. Therefore, studying and comprehending the intricacies of cervical fascial spaces through modern imaging techniques is essential. This knowledge aids in preoperative planning, intraoperative guidance, and ensuring protection through the fascial space during ablation.

However, the majority of "spaces" within the body are essentially "potential spaces," challenging their visualization through imaging and impeding in vivo research. Previous studies on fascial spaces have predominantly focused on animals or cadavers. In contrast, drawing from our extensive experience with over a thousand cases of thermal ablation for thyroid tumors[6], we observed that distinct fascial spaces become clearly visible on US following hydrodissection. Hydrodissection, commonly employed to separate the thyroid lobe and vital surrounding structures, enhances the safety of thermal ablation[6–8]. Most fascial spaces visualized on US align with anatomical structures, and a few novel spaces were discovered in this study. Consequently, this study systematically outlines the ultrasonic manifestations, boundaries, adjacent structures, and content of perithyroid

[1]Department of Interventional Medicine, China-Japan Friendship Hospital, No. 2 Ying-hua-yuan East Street, Chao-yang district, Beijing 100029, China. [2]Department of Pathology, China-Japan Friendship Hospital, Beijing, China. ✉email: yma301@163.com

fascial spaces post-hydrodissection. The confirmation of these visualizations through anatomical comparison provides a novel approach and outlook for studying fascial space visualization in vivo.

## Materials and methods

### Patients

This retrospective study received approval from the Human Ethics Review Committee of China-Japan Friendship Hospital. It was performed in compliance with the relevant guidelines and regulations. All patients provided written informed consent before undergoing ablation, and the necessity for individual informed consent for study inclusion was waived to ensure confidentiality of personal details. This study involving human participants was conducted in accordance with the ethical principles outlined in the Declaration of Helsinki.

From March 2015 to March 2022, a total of 2390 patients underwent microwave ablation for thyroid tumors at our center. Over time, experience has been accumulated, leading to the establishment of standardized hydrodissection based on perithyroid fascial spaces to mitigate complications. In this study, we retrospectively reviewed the clinical data of patients who underwent MWA with this standardized hydrodissection approach.

The inclusion criteria were as follows: (i) patients with pathologically confirmed benign symptomatic thyroid nodules or papillary thyroid carcinoma/ cervical metastatic lymph nodes; (ii) patients who either refused or were ineligible for surgery; and (iii) patients with a follow-up time of ≥ 3 months. The exclusion criteria were (i) patients with a history of cervical surgery; and (ii) patients lacking complete follow-up data.

### Preablation assessment

A LOGIQ E9 ultrasound system (GE Healthcare, Waukesha, WI) fitted with an 8.4-9 MHz linear probe was employed for puncture guidance and imaging assessments. The nodules' location, as well as their size, were meticulously measured and recorded.

### Strategy and standardization of hydrodissection

Various spaces encompass the thyroid lobe: the anterior cervical space (between infrahyoid muscles and thyroid), pretracheal space (between thyroid and trachea), retropharyngeal space (behind pharynx and thyroid), and carotid space (containing major vessels and nerves). Prior to ablation, hydrodissection strategies were applied to the respective spaces based on the nodules' locations. The choice for single or multiple fascial space hydrodissection is determined by nodule's location. In all cases, continuous injection of isolating fluid is performed until achieving a minimum protective margin of 5 mm from vital structures[7], ensuring safe and effective ablation.

Before initiating hydrodissection, a subcutaneous injection of 1% lidocaine was administered at the intended puncture site. Subsequently, an 18 G core needle, connected to an extension tube, was systematically layered and guided under ultrasound (US). As the needle tip reached the designated position, normal saline (NS) was gently injected. The confirmation of correct fascial space placement relied on the NS causing space dilation and forming an anechoic area. In instances where the surrounding soft tissue or thyroid parenchyma exhibited swelling, indicating an incorrect position, the needle tip was meticulously adjusted under US guidance. Upon successful puncture of the proposed space, NS was continuously injected, and the needle tip further refined and secured at the planned position. Typically, the needle tip was positioned proximal to the thyroid capsule corresponding to the target thyroid nodule (Fig. 1).

### Definition of fascial spaces on US

In this study, a successfully hydrodissected fascial space was characterized on US by the following features: (i) a distinct and smooth border; (ii) the ability to impede fluid flow; (iii) the formation of an anechoic or mixed-echoic isolating band upon injection, pushing critical structures away from the thyroid lobe; and (iv) liquid diffusion extent precisely aligning with the anatomical fascial space. All identified fascial spaces in this study underwent a comparative analysis with anatomical images. Given the challenge of obtaining complete cross-section specimens of the human neck, anatomical validation was conducted through systematic comparison

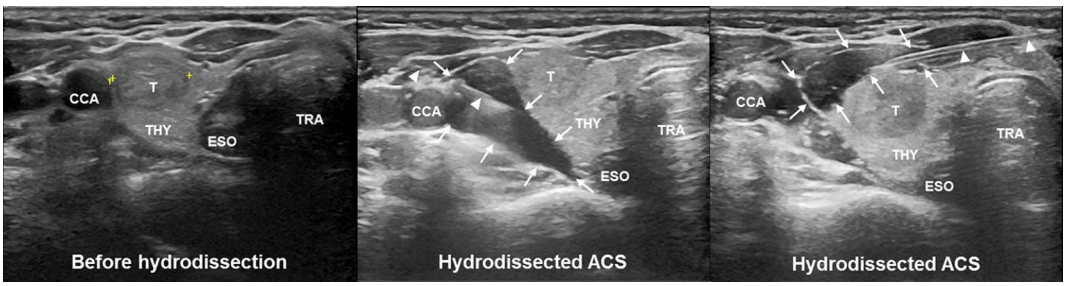


**Fig. 1**. The procedure of fascial space hydrodissection. A hypoechoic nodule located in the left lobe of the thyroid on US, positioned adjacent to the anterolateral capsule. After injection of NS along 18 G core needle (white arrowheads), the ACS (white arrows) were hydrodissected to protect the vital structures around the tumor. THY = thyroid; ESO = esophagus; TRA = trachea; CCA = common carotid artery; T = tumor; ACS = anterior cervical space.

with three reference sources: standard anatomical textbooks (Gray's Anatomy, 2008), documented cross-sectional images from published literature, and available pathological specimens from our surgical cases. For each type of fascial space identified in our study, we performed detailed anatomical comparisons to verify structural alignment and spatial relationships. Recorded US images of the hydrodissected fascial spaces were preserved for subsequent analysis.

### MWA procedure

MWA procedures were conducted under the guidance of US, following methodologies outlined in previous studies[6,9]. After ablation, the isolation fluid was gradually absorbed by the lymphatic system.

After ablation, the process of isolating fluid absorb was further researched through mixing contrast agent into isolating fluid (Sonazoid, Daiichi-Sankyo, Tokyo, Japan).

Figure 2 shows the process of absorption of the isolating fluid containing contrast agent by the perithyroid lymphatic vessels.

### Statistical methods

Statistical analyses were conducted using SPSS version 20.0 (IBM, Armonk, NY, USA). For data with a normal distribution, results were expressed as the mean ± standard deviation (SD), while for non-normally distributed data, the median and the interquartile range (IQR) of 25–75% were utilized.

## Results

A comprehensive review was conducted on 2390 patients, comprising 631 males and 1759 females, with a median age of 46 years (25–75% IQR: 26–69, age range 9–88). The nodules included 1436 benign nodules and 954 papillary thyroid carcinomas (PTCs). Hydrodissection was considered successful when it achieved three specific criteria: (1) clear visualization of the target fascial space with distinct boundaries on ultrasound, (2) establishment of a minimum 5 mm protective margin between the thyroid nodule and surrounding critical structures, and (3) stable maintenance of the isolating fluid within the intended fascial compartment. All 2390 cases in this study met these criteria. Isolating fluid was injected into various spaces, including the anterior cervical space in 1397/2390 (58.5%) cases, the pretracheal space in 1716/2390 (71.8%) cases (including 196 cases involving Berry's ligament), the retropharyngeal space in 1044/2390 (43.7%) cases, the carotid space in 28/2390 (1.2%) cases, the perilymphatic space in 98/2390 (4.1%) cases, and the tracheoesophageal groove space in 88/2390 (3.7%) cases. The subsequent sections elaborate on the distinct characteristics of these various fascial spaces.

### Anterior cervical space

*Ultrasonic characteristics post-hydrodissection*

Following hydrodissection, the anterior cervical space undergoes expansion, creating an irregular area filled with anechoic isolating fluid. The boundary is formed by the pretracheal fascia, infrahyoid fascia, and alar fascia.

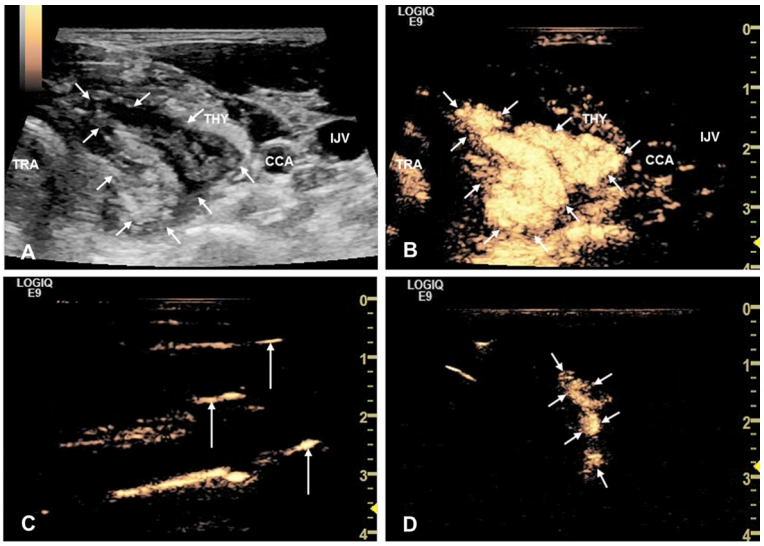


**Fig. 2**. The absorption of the isolating fluid through perithyroid lymphatic vessels. (**A**) On B-mode US, the pretracheal space (short arrows) between the trachea and the lateral lobe of thyroid showed a triangular anechoic region. (**B**) On CEUS, the pretracheal space (short arrows) was perfused by contrast agent, displaying as hyperperfusion area. (**C**) On CEUS, the enhanced perithyroid lymphatic vessels (long arrows) displayed as liner structures, which demonstrated that the contrast agent, as well as the isolating fluid was absorbed through lymphatic system. (**D**) Thirty minutes later, the range of hydrodisection area in pretracheal space (short arrows) became smaller. THY = thyroid; TRA = trachea; CCA = common carotid artery; IJV = internal jugular vein; US = ultrasound; CEUS = contrast-enhanced ultrasound.

Notably, the middle segment of the spinal accessory nerve at the lateroposterior border of the sternocleidomastoid muscle is prominently visible within this fascial space. The isolating fluid in the anterior cervical space exhibits free flow from the head side to the tail side, and it can even traverse from the ipsilateral side to the contralateral side.

*Anatomic relationships*
The anterior cervical space abuts with the infrahyoid muscles anteriorly, the thyroid gland/alar fascia posteriorly, and the carotid sheath laterally[10].

*Corresponding anatomical anterior cervical space*
The ultrasonically hydrodissected anterior cervical space aligns with the anatomical anterior cervical space (Fig. 3A).

## Pretracheal space

*Ultrasonic characteristics post-hydrodissection*
Following hydrodissection, the pretracheal space is widened by anechoic isolating fluid and manifests as a narrow band-like area situated between the trachea and the thyroid isthmus in transverse-sectional US. The pretracheal space between the trachea and the lateral lobe of the thyroid appears as a semicircular arc or triangular anechoic region. The boundary of this space is defined by the pretracheal fascia, tracheal adventitia, and buccopharyngeal fascia. Within this fascial space, various structures such as the esophagus, parathyroid, recurrent laryngeal nerve, superior laryngeal nerve, and large pretracheal lymph nodes are encompassed. Notably, at the level of the Berry ligament (C6 level), hydrodissection of the pretracheal space is impeded due to the dense structure of the ligament. The isolating fluid within the pretracheal space exhibits a superior-to-inferior flow pattern.

*Anatomic relationships*
The pretracheal space abuts the trachea posteromedially, the thyroid anterolaterally, and the retrophayngeal space/longus colli/sympathetic trunk posteriorly. At the C6 level, Berry's ligament is located laterally.

*Corresponding anatomical pretracheal space*
The ultrasonic hydrodissected pretracheal space aligns with the anatomical pretracheal space (Fig. 3B and C).

## Retropharyngeal space

*Ultrasonic characteristics -post-hydrodissection*
Following hydrodissection, the retropharyngeal space undergoes expansion, manifesting as an irregularly anechoic isolating band. Its boundaries are demarcated by the anterior buccopharyngeal fascia, posterior prevertebral fascia, and posterolateral alar fascia.

*Anatomic relationships*
The retropharyngeal space abuts the thyroid anteriorly, the carotid sheath laterally, and the prevertebral space posteriorly[11].

*Corresponding anatomical retropharyngeal space*
The ultrasonic hydrodissected retropharyngeal space aligns with the anatomical retropharyngeal space (Fig. 3D).

## Carotid space

*Ultrasonic characteristics post-hydrodissection*
Following hydrodissection, the carotid space expands, creating a circular area where anechoic isolating fluid effectively separates various structures, including the carotid artery, internal jugular vein, vagus nerve, and lymph nodes. A small amount of mixed-echoic fatty tissue is interspersed within the carotid space, and injecting isolating fluid into this tissue induces swelling. When lymph nodes are situated within adipose tissue, the fascia enveloping them can be distinctly separated into multiple layers under tension, forming a perilymphatic space. The hyperechoic fasciae, intermingled with anechoic isolating fluid, give rise to "onion skin" signs encircling the lymph node. Fluid within the carotid space exhibits free flow from the superior to the inferior area, and isolating fluid surrounding the lymph nodes gradually diffuses into adjacent fascial spaces.

*Anatomic relationships*
The carotid space abuts the thyroid gland medially, the scalene muscle laterally, the infrahyoid muscle group anteriorly, and the longus colli posteriorly.

*Corresponding anatomical carotid space*
The ultrasonically hydrodissected carotid space aligns with the anatomical carotid sheath structure. The perilymphatic space corresponds to surgically removed lymph node specimens (Fig. 4).

## Tracheoesophageal groove space

*Ultrasonic characteristics post-hydrodissection*
Following hydrodissection, the tracheoesophageal groove space undergoes edematous changes, creating a semicircular multilayer structure that presents as a mixed-echoic isolating band. In contrast to its anterolateral adjacent pretracheal space, which is filled with anechoic isolating fluid, this area predominantly exhibits a mixed

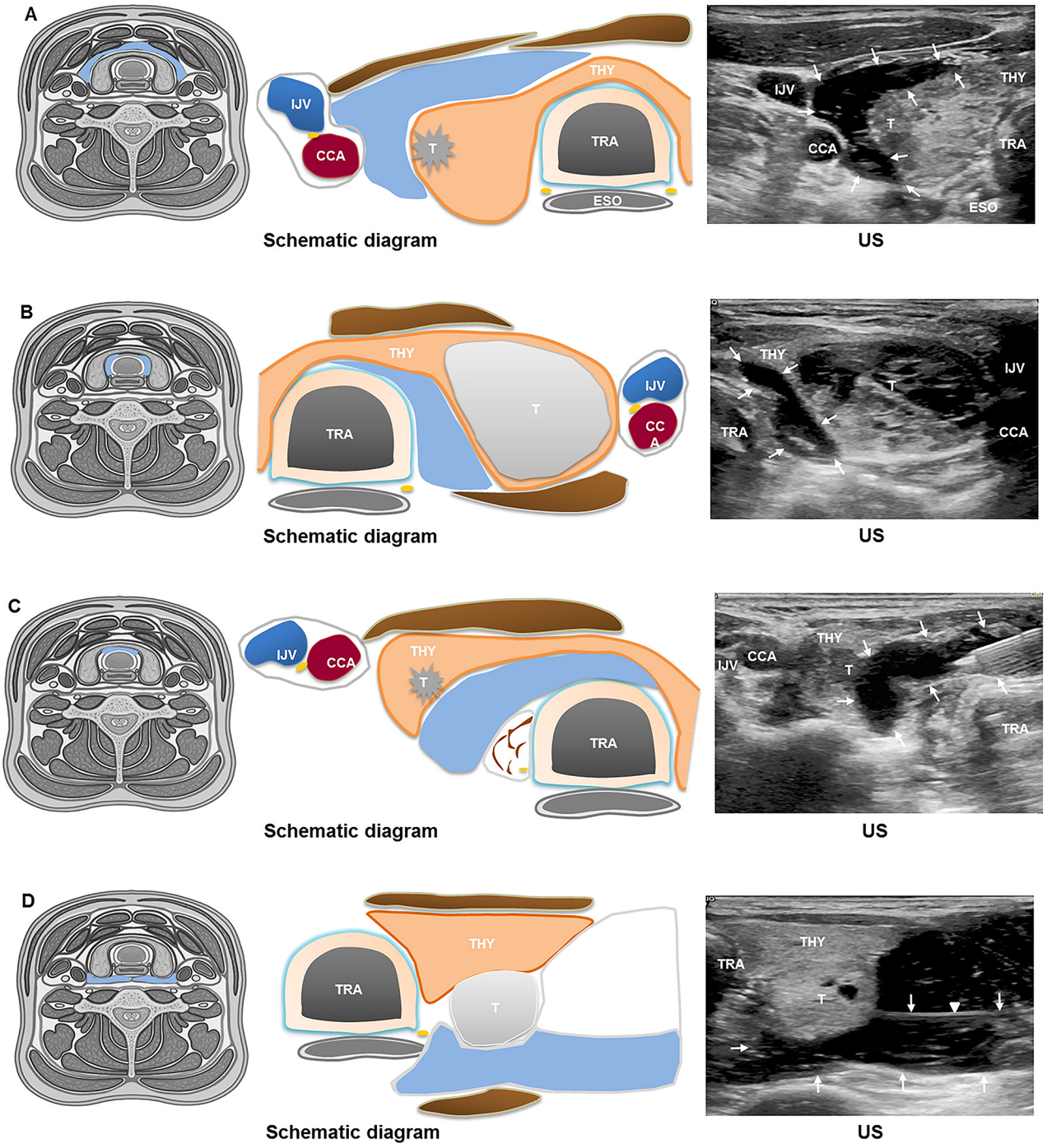


**Fig. 3**. US visualization of fascial spaces (white arrows) around thyroid after hydrodissection. (**A**) The schematic diagram of hydrodissected anterior cervical space (blue area). The US visualization of anterior cervical space (white arrows) after hydrodissection, which showed an irregularly anechoic area. (**B**) The schematic diagram of hydrodissected pretracheal space (blue area). The US visualization of pretracheal space (white arrows) after hydrodissection, which showed a semicircular arc area between the trachea and the lateral lobe of thyroid. (**C**) The schematic diagram of hydrodissected pretracheal space (blue area). The US visualization of pretracheal space (white arrows) after hydrodissection, which showed an anechoic narrow band between the trachea and the isthmus of thyroid. (**D**) The schematic diagram of hydrodissected retropharyngeal space (blue area). The US visualization of retropharyngeal space (white arrows) after hydrodissection, which showed an irregularly anechoic band. The lateral side of retropharyngeal space is the alar fascia (white arrowhead). THY = thyroid; ESO = esophagus; TRA = trachea; CCA = common carotid artery; IJV = internal jugular vein; T = tumor; US = ultrasound.

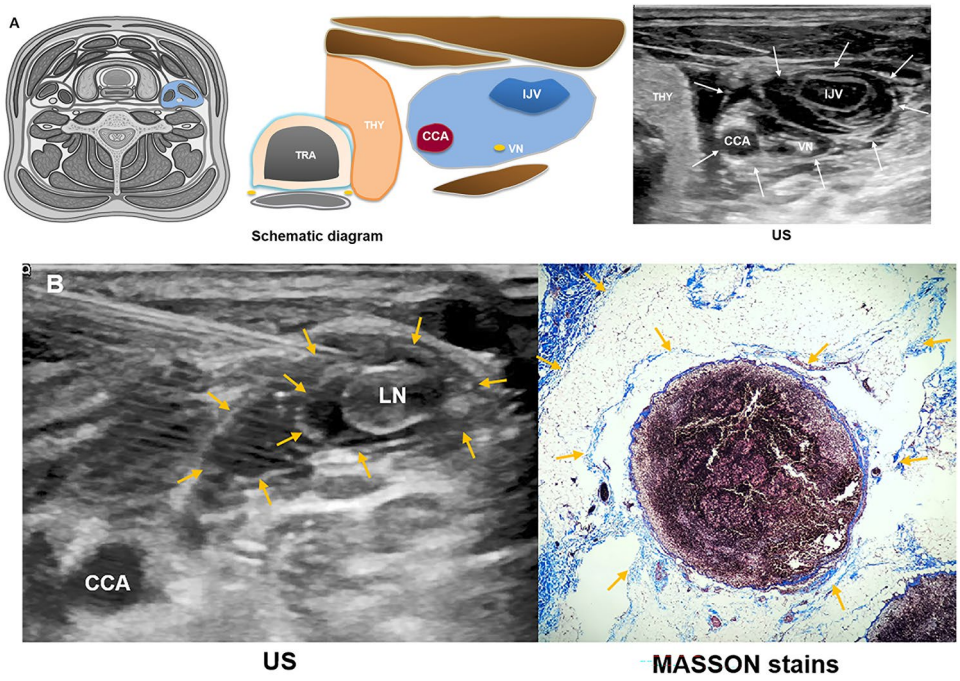


**Fig. 4**. (**A**) The schematic diagram of hydrodissected carotid space (blue area). The US visualization of carotid space after hydrodissection, which showed a circular anechoic area (white arrows); carotid artery (CCA), internal jugular vein (IJV) and vagus nerve (VN) are fully separated by isolating fluid. (**B**) The "onion skin" sign emerged after injection of NS beside lymph node, which gave the proof that there was cyclic space (yellow arrows) around lymph node. The MASSON stains of postoperative specimen showed there was indeed several layers of circular distributed collagen fibers (yellow arrows) around lymph node, which demonstrated there was cyclic spaces wrapped lymph node. LN = lymph node; CCA = common carotid artery; IJV = internal jugular vein; VN = vagus nerve; US = ultrasound.

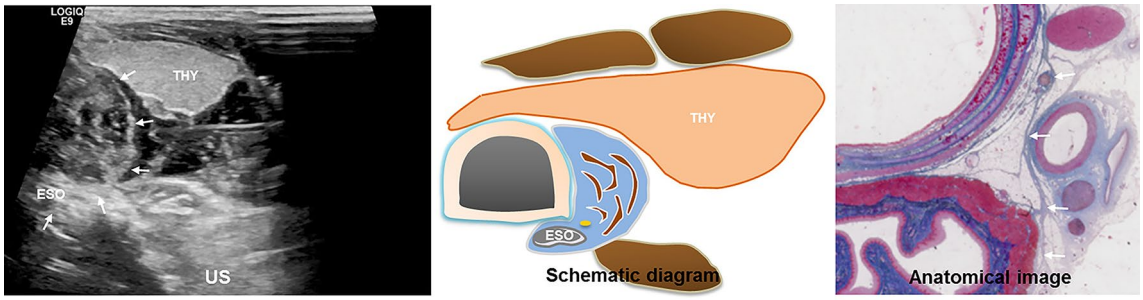


**Fig. 5**. The US visualization of tracheoesophageal groove space (white arrows), which showed a semicircular multilayer mixed-echoic area. The schematic diagram of hydrodissected tracheoesophageal groove space (blue area). According to anatomical image reported, there was continuing collagenous fiber (white arrows) wrapped tracheoesophageal and groove, which confirmed the tracheoesophageal groove space. THY = thyroid; ESO = esophagus; US = ultrasound.

echo with a distinct border and tension. The anechoic fluid is confined and gradually diffuses within, while the adipose tissue appears hyperechoic. Notably, the recurrent laryngeal nerve is situated within this fascial space.

*Anatomic relationships*
The tracheoesophageal groove space abuts the trachea laterally and the pretracheal space medially.

*Corresponding anatomical tracheoesophageal groove space*
The tracheoesophageal groove space emerges as a refined fascial space following hydrodissection. While this space has not been anatomically reported, the corresponding fascial structure has been identified in previously reported anatomical images (Fig. 5).

Post-ablation, the absorption of isolating fluid through the lymphatic system was closely observed within a 60-minute timeframe (Fig. 2).

## Discussion

The anatomy of the neck is relatively complex, housing numerous critical structures and potential fascial spaces that either separate or envelop different anatomical components. These potential fascial spaces are encased in a continuous network of fibrous connective tissue, often interspersed with fatty tissue and essential structures like organs, blood vessels, nerves, and lymph nodes. Notably, adjacent fascial spaces may originate from distinct germ layers[12], maintaining a relatively independent existence while interconnected to form continuous functional bodies.

The fascial spaces have vital pathophysiological significance, such as forming the basic environment for organ activity, building a line of defense for organs and confining or spreading inflammation. In clinical settings, these spaces frequently serve as essential anatomical landmarks for precise surgical dissection and for targeting fascia plane blocks[13,14]. Consequently, a deeper comprehension and effective application of the various fascial spaces adjacent to the target tumor during surgery can significantly minimize injury. This is achieved through the accurate isolation and resection along the specific fascial space in close proximity. However, because the fascial space is a potential space, it can only be displayed under gross anatomy and microscopy, and cannot be clearly identified on imaging. Currently, there is a limited number of studies focusing on the clear visualization and precise manipulation of the fascial space in vivo.

The present study demonstrates that accurate injection of NS allows for the visualization of perithyroid fascial spaces using US. The key findings can be summarized as follows(i) Each fascial space exhibits a distinct and consistent shape, closely associated with its internal inherent structure and boundaries. (ii) Variability exists in the contents of different fascial spaces, some containing minimal amounts of fat while others house significant structures. (iii) Different fascial spaces demonstrate diverse modes of isolating fluid dispersion. Some exhibit free-flowing characteristics, while others display slow diffusion, and some reveal fat swelling. (iv) Expanded fascial spaces effectively separate surrounding structures, with varying distances achieved through different injection pressures. (v) The pressure characteristics within the fascial space are reflected by the flow and diffusion direction of NS. (vi) Large intrinsic fascial spaces can encompass several small spaces surrounding minute structures, such as the perilymphatic space and tracheoesophageal groove space.

In this study, the majority of the identified fascial spaces align with conventional anatomical spaces. Notably, a few spaces were revealed for the first time through the use of US, consistent with the characteristic nature of fascial spaces on US imaging. Although these particular fascial spaces may not be explicitly documented in traditional anatomy, our observations indicate that corresponding fascial structures do exist in the anatomical context. The distribution of fascia observed on US corresponds to these spaces, exemplified by findings such as the perilymphatic space and the tracheoesophageal groove space. Furthermore, the apparent absence of certain fascial spaces in traditional anatomical descriptions may be attributed to the limitation of visualizing these spaces through conventional imaging techniques.

In clinical settings, the hydrodissection technique serves as a protective measure to mitigate heat-related injury to adjacent structures during the thermal ablation of thyroid tumors or cervical lymph nodes[8,15]. Moreover, the application of hydrodissection introduces a novel avenue for investigating fascial spaces. This technique offers several advantages: (i) The minimally invasive nature of US-guided injection of isolating fluid through a fine needle allows for routine visualization of fascial spaces. (ii) The physicochemical properties of NS as the isolating fluid closely resemble the body's microenvironment, ensuring minimal risk of injury or post-procedural adhesion. (iii) Following hydrodissection, the expanded fascial space is filled with NS, facilitating clear visualization on US and establishing a foundation for subsequent studies.

Beyond these technical advantages, the hydrodissection technique combined with contrast agents demonstrates potential clinical applications beyond thermal ablation. The visualization of Sonazoid absorption through perithyroid lymphatic vessels (Fig. 2) effectively traces lymphatic drainage patterns. This finding aligns with our previous studies[16,17], which demonstrated that enhanced lymphatic imaging improves metastatic lymph node detection. Additionally, the anatomical characterization of fascial planes through contrast agent distribution corresponds with recent advances in fascial plane blocks, as documented by Xu et al.[18]. Building upon Back et al.'s research on lymphatic mapping patterns[19], future research directions may explore the feasibility of combining this technique with alternative contrast agents for lymph node imaging, aiming to develop standardized protocols for preoperative planning and assessment of cervical lymph node metastasis.

Nevertheless, several limitations need to be acknowledged. First, the technique requires further standardization across different anatomical variations. Second, the current US imaging resolution may limit the detection of microscopic structures. Third, the visualization of fascial spaces would benefit from direct comparison with comprehensive cross-sectional specimens for anatomical validation.

## Conclusion

The visualization of the fascial space can be achieved through the guided injection of NS into the fascial spaces using US. The systematic implementation of hydrodissection strategies not only guarantees the safety and efficacy of thermal ablation procedures but also paves the way for future in vivo studies on the physiology and pathology of the fascial microenvironment.

## Data availability

The data that support the findings of this study are not openly available due to reasons of sensitivity and are available from the corresponding author upon reasonable request.

Received: 21 January 2024; Accepted: 28 January 2025
Published online: 06 February 2025

## References

1. Langevin, H. M. & Huijing, P. A. Communicating about fascia: history, pitfalls, and recommendations. *Int. J. Ther. Massage Bodyw.* **2**, 3–8. https://doi.org/10.3822/ijtmb.v2i4.63 (2009).
2. Editor, S. S. *Gray's Anatomy: the anatomical basis of clinicalpractice* (Elsevier Churchill Livingstone, 2008).
3. Verlag, S. G. T. Federative International Programme on Anatomical Terminologies [FIPAT] (eds.), Terminologia Anatomica: international anatomical terminology (2nd ed.). ed., (2011).
4. Stedman, S. Stedmans Medical Dictionary, 28 edition ed., Lippincott Williams & Wilkins, (2006).
5. Adstrum, S., Hedley, G., Schleip, R., Stecco, C. & Yucesoy, C. A. Defining the fascial system. *J. Bodyw. Mov. Ther.* **21**, 173–177. https://doi.org/10.1016/j.jbmt.2016.11.003 (2017).
6. Cao, X. J. et al. Efficacy and safety of thermal ablation for treatment of Solitary T1N0M0 papillary thyroid carcinoma: a Multicenter Retrospective Study. *Radiology* **300**, 209–216. https://doi.org/10.1148/radiol.2021202735 (2021).
7. Zhao, Z. L. et al. Upgraded hydrodissection and its safety enhancement in microwave ablation of papillary thyroid cancer: a comparative study. *Int. J. Hyperth.* **40**, 2202373. https://doi.org/10.1080/02656736.2023.2202373 (2023).
8. Wei, Y. et al. Microwave ablation versus Surgical Resection for Solitary T1N0M0 papillary thyroid carcinoma. *Radiology* **212313** https://doi.org/10.1148/radiol.212313 (2022).
9. Zhuo, L. et al. US-guided microwave ablation of hyperplastic parathyroid glands: safety and efficacy in patients with end-stage renal Disease-A pilot study. *Radiology* **282**, 576–584. https://doi.org/10.1148/radiol.2016151875 (2017).
10. Parker, G. D., Harnsberger, H. R. & Smoker, W. R. The anterior and posterior cervical spaces, Semin. *Ultrasound Ct Mri.* **12**, 257–273 (1991).
11. Som, C. H. *PM, Head and neck Imaging* (Elsevier Mosby, 2011).
12. Mansberger, A. J. & Wei, J. P. Surgical embryology and anatomy of the thyroid and parathyroid glands. *Surg. Clin. -North Am.* **73** https://doi.org/10.1016/s0039-6109(16)46082-2 (1993). 727 – 46.
13. Gamss, C., Gupta, A., Chazen, J. L. & Phillips, C. D. Imaging evaluation of the suprahyoid neck. *Radiol. Clin. N Am.* **53**, 133–144. https://doi.org/10.1016/j.rcl.2014.09.009 (2015).
14. Warshafsky, D., Goldenberg, D. & Kanekar, S. G. Imaging anatomy of deep neck spaces. *Otolaryngol. Clin. N Am.* **45**, 1203–1221. https://doi.org/10.1016/j.otc.2012.08.001 (2012).
15. Qiu, Y. et al. Ultrasound-guided thermal ablation for cervical lymph node metastasis from thyroid carcinoma: a meta-analysis of clinical efficacy and safety. *Lasers Med. Sci.* **37**, 1747–1754. https://doi.org/10.1007/s10103-021-03428-5 (2022).
16. Wei, Y. et al. Effectiveness of lymphatic contrast enhanced Ultrasound in the diagnosis of cervical lymph node metastasis from papillary thyroid carcinoma. *Sci. Rep.* **12**, 578. https://doi.org/10.1038/s41598-021-04503-1 (2022).
17. Wei, Y. et al. Combination of Lymphatic and Intravenous Contrast-Enhanced Ultrasound for Evaluation of Cervical Lymph Node Metastasis from papillary thyroid carcinoma: a preliminary study, Ultrasound Med. *Biol* **47**, 252–260. https://doi.org/10.1016/j.ultrasmedbio.2020.10.003 (2021).
18. Xu, G. et al. Ultrasound-guided superficial cervical plexus block combined with clavipectoral fascial plane block or interscalene brachial plexus block in clavicle surgery: a single-centre, double-blind, randomized controlled trial. *J. Clin. Monit. Comp.* **37**, 985–992. https://doi.org/10.1007/s10877-022-00968-1 (2023).
19. Back, K. et al. Optimal value of lymph node ratio and metastatic lymph node size to predict risk of recurrence in pediatric thyroid cancer with lateral neck metastasis. *J. Pediatr. Surg.* **58**, 568–573. https://doi.org/10.1016/j.jpedsurg.2022.07.010 (2023).

## Author contributions

Guarantors of integrity of entire study, W.Y., Y.M.A.; study concepts/study design or data acquisition or data analysis/interpretation, all authors; manuscript drafting or manuscript revision for important intellectual content, W.Y., Y.M.A., Z.Z.L.; approval of final version of submitted manuscript, all authors; agrees to ensure any questions related to the work are appropriately resolved, all authors; literature research, W.Y.; clinical studies, W.Y.,Y.M.A.,Z.Z.L., P.L.L., L.Y.; pathological studies, N.Y.; statistical analysis, W.Y.; and manuscript editing, W.Y., Y.M.A., Z.Z.L.

## Declarations

## Competing interests

The authors declare no competing interests.

## Additional information

**Correspondence** and requests for materials should be addressed to M.-a.Y.

**Reprints and permissions information** is available at www.nature.com/reprints.

**Publisher's note** Springer Nature remains neutral with regard to jurisdictional claims in published maps and institutional affiliations.